Journal of Computational Applied Mechanics 2026, 57(1): 11-26

DOI: 10.22059/jcamech.2025.402334.1612

RESEARCH PAPER

Thermoelastic plane strain solutions to rotating cylinders due to a refined fractional-order theory

Ashraf M. Zenkour [a,b,*], Tareq Saeed [a,c], Abdullah A. Almalki [a]

[a] *Department of Mathematics, Faculty of Science, King Abdulaziz University, P.O. Box 80203, Jeddah 21589, Saudi Arabia*
[b] *Department of Mathematics, Faculty of Science, Kafrelsheikh University, Kafrelsheikh 33516, Egypt*
[c] *Financial Mathematics and Actuarial Science (FMAS)-Research Group, Department of Mathematics, Faculty of Science, King Abdulaziz University, Jeddah 21589, Saudi Arabia*

Abstract

This article develops a fractional-order Lord-Shulman (LS) generalized thermoelastic model to analyze a rotating hollow cylinder under plane strain. The cylinder, with traction-free surfaces, is subjected to non-uniform ramp-type heating on its outer boundary. Governing equations incorporating non-Fourier heat conduction are solved using the Laplace transform technique with numerical inversion. Results for temperature, displacement, stress, and dilatation are computed and graphically presented. The analysis demonstrates that both the fractional-order and ramp-time parameters significantly influence the thermoelastic response. Comparisons with classical Fourier-based theory highlight the model's accuracy in capturing wave propagation phenomena, providing critical insights for the design of structures experiencing sudden thermal loads.

Keywords: Rotating cylinder; plane strain; fractional-order; LS theory; wave propagation.

1. Introduction

A lot of referenced papers explore coupled thermoelasticity and generalized thermoelasticity in cylindrical systems, focusing on transient thermal stresses, dynamic responses, and nonlinear material behavior. Biot [1] introduced coupled thermoelasticity, resolving the classical paradox where mechanical deformation did not affect temperature. Yang and Chen [2] solved 1D axisymmetric transient thermoelastic problems with thermo-mechanical coupling in terms of temperature and displacement. Jane and Lee [3] analyzed multilayered cylinders under thermal loads using Laplace transforms and finite difference methods. Lee et al. [4] extended solutions to orthotropic multilayered cylinders under quasi-static thermoelastic conditions. Lee [5] developed methods for 3D axisymmetric problems in nonhomogeneous cylinders of varying lengths. Gaikwad et al. [6] studied temperature, displacement, and stress in cylinders with arbitrary surface heating. Zenkour et al. [7] compared thermoelastic plate theories (classical, Lord-Shulman, Green-Lindsay) for functionally graded plates under thermal loads. Hung et al. [8] analyzed initial interface pressure in heat-assembled cylinders, providing a computational method for quasi-static thermoelastic problems. Eskandari-Ghadi et al. [9] solved 2D dynamic thermoelasticity using potential functions to uncouple governing equations. Zenkour and Abbas [10] studied nonlinear transient stresses in temperature-dependent cylinders under time-decaying thermal fields.

* Corresponding author. Tel.: +966-054-005-5690.
E-mail address: zenkour@kau.edu.sa

One of the most significant generalized thermoelasticity models (hyperbolic heat conduction) is the Lord and Shulman (LS) one. They [11] introduced a finite thermal wave speed model, eliminating the paradox of infinite heat propagation. Dhaliwal and Sherief [12] extended LS model to anisotropic materials. Sherief and Anwar [13] and Youssef [14, 15] applied it to cylindrical cavities with ramp-type heat and temperature-dependent assets. Marchi and Zgrablich [16] developed a finite integral transform for radiation boundary conditions. Various methods (potential functions, computational schemes) addressed multiphysics coupling in thermoelastic systems. Sherief and Anwar [13] solved thermoelasticity problems for an infinitely long hollow cylinder with temperature-boundary conditions and traction-free surfaces using the LS theory (one relaxation time). Youssef [14] derived generalized thermoelasticity equations for temperature-dependent materials, incorporating variable mechanical/thermal properties under the LS model. Youssef [15] analyzed transient thermoelastic relations in an unbounded medium with a cylindrical cavity under mechanical loading and starting from rest.

Several studies analyzed thermoelastic interactions in different cylindrical geometries (unbounded media with cavities, hollow cylinders, and annular cylinders) using generalized thermoelasticity theories (mainly the LS model). Youssef [17] presented thermoelastic disturbances in a half-space with a cylindrical cavity. Abo-Dahab and Abbas [18] presented magneto-thermoelastic transient effects with variable thermal conductivity. Elhagary [19] discussed thermoelastic diffusion (coupled heat and mass transfer) in a hollow cylinder. Zenkour and Abbas [20] presented temperature-dependent material assets in an annular cylinder under thermal stress. Abbas and Elmaboud [21]compared exact and approximate (homotopy analysis) solutions for hollow cylinders, showing good agreement. Zenkour [22] studied variable thermal conductivity in clamped hollow cylinders under thermal shock, highlighting its impact on stress distribution. Youssef and El-Bary [23] analyzed semiconducting viscothermoelastic cylinders with laser-induced heating, coupling thermal, elastic, and charge carrier effects. Eker and Yarımpabuç [24] examined thick-walled cylinders with transient heating, revealing stress waves due to LS theory.

Recent research in generalized thermoelasticity has focused on Green and Lindsay (GL) and Green and Naghdi (GN) models to study thermal and mechanical wave propagation in hollow cylinders and axisymmetric structures. Green and Lindsay (GL) [25] incorporated two relaxation times to account for thermal and mechanical wave propagations. Green and Naghdi (GN) models [26-28] of type I (classical thermoelasticity with Fourier heat conduction), type II (thermoelasticity without energy dissipation, involving hyperbolic heat conduction), and type III (generalized model combining features of types I and II) are all included. Allam et al. [29] studied thermal stress in a homogeneous isotropic cylinder with a hole using GN theory. Zenkour and Abouelregal [30] examined orthotropic cylinders with cavities under GN theory. Zenkour and Kutbi [31] unified multiple-phase lags, GL, LS, and classical models in a generalized thermoelastic diffusion framework. Othman and Abbas [32] derived GN-based equations for hollow cylinders (Types II and III). Bezzina and Zenkour [33] modified the GN theory for thermoelastic diffusion in cylinders under thermal/chemical loads. Abbas and Othman [34] extended the GN II and III theories for rotating cylinders. Zenkour and Kutbi [35] applied GN theory without energy dissipation to a hollow cylinder under continuous heat sources.

Several studies have investigated the time-fractional wave equation and generalized thermoelasticity in cylindrical geometries using Caputo fractional derivatives of order $0 < \alpha \leq 2$. Povstenko [36] solved fractional diffusion-wave problems in infinite cylinders using integral transforms under Dirichlet/Neumann boundary conditions. Youssef and Al-Lehaibi [37] improved a fractional thermoelastic model for materials with a cylindrical cavity. Abouelregal [38] studied an infinite solid cylinder using fractional heat conduction with one relaxation time. Khamis et al. [39] analyzed thermoelastic interactions in an infinite medium with a cavity using fractional strain theory. Said et al. [40] introduced a multi-phase-lag fractional model for a hollow cylinder, incorporating magnetic fields and rotation. Xie and He [41] examined a rotating hollow conductor under thermal shock using memory-dependent derivatives and variable material properties. Al-Lehaibi [42] introduced a hyperbolic two-temperature model for an annular cylinder, incorporating fractional-order strain theory and thermal shock conditions. Othman and Atef [43] derived fractional heat conduction equations using Riemann-Liouville and Caputo derivatives. Warbhe and Gujarkar [44] analyzed time-fractional heat transfer in a hollow cylinder using the Caputo derivative. Zhu et al. [45] studied a hollow cylinder with variable thermal properties under fractional thermoelastic diffusion. Adel et al. [46] examined the Moore-Gibson-Thompson (MGT) effect on moisture diffusion in semiconductors. Sherief and Hussein [47] developed a fractional thermoporoelasticity theory for geomechanical applications. Zakria and Abouelregal [48] modeled viscoelastic materials with linear and nonlinear constitutive laws. Wang and Ma [49] investigated thermal shock response in a hollow cylinder using fractional viscoelasticity. Khader [50] proposed a micropolar thermoelastic model for a solid cylinder using Caputo derivatives.

In this work, a refined fractional-order thermoelastic model is developed based on the Lord-Shulman theory to analyze a rotating hollow cylinder under plane strain conditions. The cylinder, with traction-free boundaries, is subjected to ramp-type thermal heating. The governing equations incorporate non-Fourier heat conduction and are

solved using the Laplace transform technique. The results demonstrate that the distributions of temperature, displacement, and stress are highly sensitive to the fractional-order and heating-rate parameters. A comparison with classical thermoelastic theory confirms that the proposed model provides a more accurate representation of transient wave propagation. This work offers critical insights for the design of structures subjected to thermal shock.

2. Modified fractional-order thermoelasticity theory

In this section, a concise presentation of the constitutive and field equations for a homogeneous, isotropic elastic body under the fractional-order generalized thermoelasticity theory (based on LS theory with fractional derivatives):

1. Equation of motion:

$$\frac{\partial \sigma_r}{\partial r} + \frac{\sigma_r - \sigma_\theta}{r} + \rho\omega^2 r = 0, \tag{1}$$

where ρ is the material density of the rotating cylinder, σ_r and σ_θ are the radial and circumferential (hoop) stresses, ω is the angular frequency, and (r, θ, z) are the cylindrical coordinates system.

2. Time-fractional heat conduction equation:

The generalized heat conduction equation with fractional derivative heat transfer stretched by the refined form of Lord and Shulman [11] (F-LS (r)) theory is

$$\kappa\nabla^2\phi = \mathcal{D}\left[\rho c_\vartheta \frac{\partial \phi}{\partial t} + \gamma T_0 \frac{\partial \varepsilon}{\partial t} - Q\right], \tag{2}$$

where κ represents the thermal conductivity, c_ϑ is the specific heat at fixed strain, $Q(r,t)$ is the heat source, and $\varepsilon = \nabla \cdot \vec{u}$ is dilatation with the displacement vector $\vec{u} \equiv (u_r, 0, u_z)$. Also, $\phi = T - T_0$ represents the temperature increment wherein T_0 is the reference temperature, and $T(r,t)$ is the absolute temperature. For the present plane strain problem, the coupling parameter γ is given by

$$\gamma = \frac{\alpha E}{1-2\nu}, \tag{3}$$

where E denotes Young's modulus, ν is Poisson's ratio, and α denotes the linear parameter of thermal expansion in Eq. (2), ∇^2 represents the Laplacian in the cylindrical coordinates, and $\mathcal{D}$ is a differential parameter. They are given by

$$\nabla^2 = \frac{\partial^2}{\partial r^2} + \frac{1}{r}\frac{\partial}{\partial r}, \quad \mathcal{D} = 1 + \sum_{n=1}^{N} \frac{\tau^{n+\beta}}{(n+\beta)!}\frac{\partial^{n+\beta}}{\partial t^{n+\beta}}, \quad N \geq 1, \tag{4}$$

where τ is the first relaxation time and β is the fractional order parameter $(0 < \beta \leq 1)$.

The simple heat conduction equation with fractional derivative (FD (s)) heat transfer in the context of Eq. (2) can be reduced to (neglecting the summation)

$$\kappa\nabla^2\phi = \left(1 + \frac{\tau^\beta}{\alpha!}\frac{\partial^\beta}{\partial t^\beta}\right)\left[\rho c_\vartheta \frac{\partial \phi}{\partial t} + \gamma T_0 \frac{\partial \varepsilon}{\partial t} - Q\right], \quad 0 < \beta \leq 1. \tag{5}$$

It is clear that the case of $\beta = 1$ in Eq. (4) represents the simple Lord and Shulman (LS (s)) theory

$$\kappa\nabla^2\phi = \left(1 + \tau\frac{\partial}{\partial t}\right)\left[\rho c_\vartheta \frac{\partial \phi}{\partial t} + \gamma T_0 \frac{\partial \varepsilon}{\partial t} - Q\right], \tag{6}$$

while the case of omitting β represents the classical thermoelasticity (CTE) theory

$$\kappa\nabla^2\phi = \rho c_\vartheta \frac{\partial \phi}{\partial t} + \gamma T_0 \frac{\partial \varepsilon}{\partial t} - Q. \tag{7}$$

Also, in the case of $N = 1$, one can get the generalized heat conduction equation with fractional derivative heat transfer in the simplest fractional-order form of Lord and Shulman (F-LS (s)) theory as

$$\kappa\nabla^2\phi = \left(1 + \frac{\tau^{1+\beta}}{(1+\beta)!}\frac{\partial^{1+\beta}}{\partial t^{1+\beta}}\right)\left(\rho c_\vartheta \frac{\partial \phi}{\partial t} + \gamma T_0 \frac{\partial \varepsilon}{\partial t} - Q\right), \quad 0 < \beta < 1. \tag{8}$$

Setting $\beta \to 0$ in the above equation, one can return to the LS (s) theory as in Eq. (6). However, by setting $\beta \to 0$ in Eq. (2) with the aid of Eq. (4), one can obtain the refined Lord and Shulman (LS (r)) theory in the form

$$\kappa\nabla^2\phi = \left(1 + \sum_{n=1}^{N}\frac{\tau^n}{n!}\frac{\partial^n}{\partial t^n}\right)\left(\rho c_\vartheta \frac{\partial \phi}{\partial t} + \gamma T_0 \frac{\partial \varepsilon}{\partial t} - Q\right), \quad N \geq 1. \tag{9}$$

3. Cauchy relations

The relationship between the radial displacement u_r and the strains in a rotating cylinder under plane strain conditions are purely kinematic (derived from geometry) and do not depend on material properties like thickness or density. For a cylindrically symmetric system, the strains in polar coordinates (r, θ, z) are expressed in terms of u_r as

$$\varepsilon_r = \frac{\partial u_r}{\partial r}, \quad \varepsilon_\theta = \frac{u_r}{r}, \quad \varepsilon_z = \frac{\partial u_z}{\partial z} = 0, \tag{10}$$

where ε_r, ε_θ, ε_z are the radial, hoop, and axial strains, respectively, and dilatation ε is given by

$$\varepsilon = \varepsilon_r + \varepsilon_\theta = \frac{1}{r}\frac{\partial}{\partial r}(r u_r). \tag{11}$$

This geometric condition ensures consistent deformation, leading to the following compatibility equation that must be satisfied:

$$\frac{\partial}{\partial r}(r\varepsilon_\theta) - \varepsilon_r = 0. \tag{12}$$

For the elastic deformation, the inverse Duhamel-Neumann relations for the cylinder can be described Hooke's law,

$$\begin{Bmatrix}\varepsilon_r \\ \varepsilon_\theta \\ \varepsilon_z\end{Bmatrix} = \frac{1}{E}\begin{bmatrix}1 & -\nu & -\nu \\ -\nu & 1 & -\nu \\ -\nu & -\nu & 1\end{bmatrix}\begin{Bmatrix}\sigma_r \\ \sigma_\theta \\ \sigma_z\end{Bmatrix} - \alpha\phi. \tag{13}$$

For plane-strain ($\varepsilon_z = 0$), we have

$$\sigma_z = \nu(\sigma_r + \sigma_\theta) + \alpha E\phi, \tag{14}$$

and hence, substituting it into Eq. (13) for ε_r and ε_θ, we have

$$\begin{Bmatrix}\varepsilon_r \\ \varepsilon_\theta\end{Bmatrix} = \frac{1+\nu}{E}\begin{bmatrix}1-\nu & -\nu \\ -\nu & 1-\nu\end{bmatrix}\begin{Bmatrix}\sigma_r \\ \sigma_\theta\end{Bmatrix} - (1+\nu)\alpha\phi. \tag{15}$$

Substitution of the above expressions for ε_r and ε_θ into the dilatation in Eq. (11) and into the compatibility equation in Eq. (12), respectively, one obtains

$$\varepsilon = \frac{(1+\nu)(1-2\nu)}{E}(\sigma_r + \sigma_\theta) - 2(1+\nu)\alpha\phi, \tag{16}$$

$$\frac{\sigma_r - \sigma_\theta}{r} + \nu\frac{\partial \sigma_r}{\partial r} - (1-\nu)\frac{\partial \sigma_\theta}{\partial r} + \alpha E\frac{\partial \phi}{\partial r} = 0. \tag{17}$$

Setting

$$\sigma_r = \frac{s(r,t)}{r}, \tag{18}$$

in Eq. (1) yields

$$\sigma_\theta = \frac{\partial s}{\partial r} + \rho\omega^2 r^2. \tag{19}$$

Substituting for ε, σ_r, and σ_θ in Eqs. (17) and (2), to get the governing equations as

$$\frac{\partial^2 s}{\partial r^2} + \frac{1}{r}\frac{\partial s}{\partial r} - \frac{s}{r^2} - \frac{\alpha E}{1-\nu}\frac{\partial \phi}{\partial r} + \frac{(3-2\nu)\rho\omega^2 r}{1-\nu} = 0. \tag{20}$$

$$\frac{\partial^2 \phi}{\partial r^2} + \frac{1}{r}\frac{\partial \phi}{\partial r} = \mathcal{D}_t\left[\frac{1}{\kappa}\left(\rho c_\vartheta - \frac{2\alpha^2 E(1+\nu)}{1-2\nu}T_0\right)\phi + \frac{(1+\nu)\alpha T_0}{\kappa}\left(\frac{\partial s}{\partial r} + \frac{s}{r}\right)\right], \quad \mathcal{D}_t = \mathcal{D}\frac{\partial}{\partial t}. \tag{21}$$

Also, the dilatation in Eq. (16) becomes

$$\varepsilon = \frac{(1+\nu)(1-2\nu)}{E}\left(\frac{\partial s}{\partial r} + \frac{s}{r} + \rho\omega^2 r^2\right) - 2(1+\nu)\alpha\phi. \tag{22}$$

3. Initial and boundary conditions

Let us consider some relations to describe the imposed initial and boundary conditions of the cylinder shown in Figure 1. On both inner and outer surfaces, the rotating cylinder is traction-free.

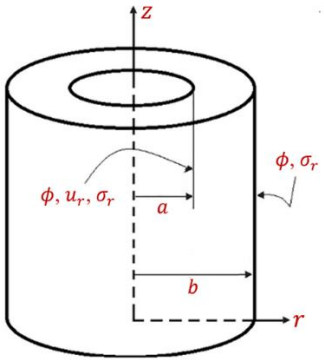

Fig 1: Schematic and geometry of the hollow cylinder

That is

$$\sigma_r(r,t)|_{r=a} = \sigma_r(r,t)|_{r=b} = 0. \tag{23}$$

Thermal loading is applied to the outer surface of the rotating cylinder, while its inner surface remains insulated. Hence, the thermal boundary conditions are stated as

$$\phi(r,t)|_{r=a} = 0, \quad \phi(r,t)|_{r=b} = g(t), \tag{24}$$

where $g(t)$ is the function of thermal loading useful to the outer surface $r = b$ of the cylinder. The ramp-type heating is utilized as

$$g(t) = \phi_0 \begin{cases} \frac{t}{t_0}, & 0 < t < t_0 \\ 1, & t \geq t_0 \end{cases}, \tag{25}$$

where $t_0 > 0$ is the parameter of ramp-type heating, and $\phi_0 > 0$ is a constant that signifies the thermal loading. Also, the inner radius of the rotating cylinder is displacement variation-free, that is

$$\left.\frac{\partial u_r(r,t)}{\partial r}\right|_{r=a} = 0. \tag{26}$$

Concerning the initial conditions, one can assume the following equations that describe the initial conditions

$$\phi(r,0) = \frac{\partial^n}{\partial t^n}\phi(r,0) = s(r,0) = \frac{\partial^n}{\partial t^n}s(r,0) = 0, \quad n = 1, 2, 3, \ldots . \tag{27}$$

4. Laplace transform

Let us apply the well-known Laplace transform given by

$$\mathcal{L}\{f(r,t)\} = \bar{f}(r,p) = \int_0^\infty f(r,t)\, \mathrm{e}^{-pt}\mathrm{d}t. \tag{28}$$

Then the governing equations in the Laplace domain are given by

$$\mathcal{D}_0\mathcal{D}_1(\bar{s}) = c_1\mathcal{D}_0(\bar{\phi}) - c_2 r, \tag{29}$$

$$(\mathcal{D}_1\mathcal{D}_0 - c_3)\bar{\phi} = c_4\mathcal{D}_1(\bar{s}), \tag{30}$$

where $\mathcal{D}_0$ and $\mathcal{D}_1$ are the two differential parameters

$$\mathcal{D}_0 = \frac{\mathrm{d}}{\mathrm{d}r}, \quad \mathcal{D}_1 = \frac{\mathrm{d}}{\mathrm{d}r} + \frac{1}{r}, \tag{31}$$

and

$$c_1 = \frac{\alpha E}{1-\nu}, \quad c_2 = \frac{(3-2\nu)\rho\omega^2}{1-\nu}, \quad c_3 = \frac{\psi}{\kappa}\left(\rho c_\vartheta - \frac{2\alpha^2 E(1+\nu)}{1-2\nu}T_0\right), \quad c_4 = \frac{(1+\nu)\alpha\psi T_0}{\kappa}. \tag{32}$$

The parameter ψ will be given according to the theory used. That is

i) The classical thermoelasticity (CTE) theory:

$$\psi = p. \tag{33}$$

ii) The simple Lord and Shulman thermoelasticity (LS (s)) theory:

$$\psi = p(1 + \tau\, p). \tag{34}$$

iii) The refined Lord and Shulman thermoelasticity (LS (r)) theory:

$$\psi = p\left(1 + \sum_{n=1}^{N} \frac{\tau^n}{n!} p^n\right). \tag{35}$$

For the present fractional order theories, if $\beta > 0$, $m = [\beta] + 1$, and if $h(t)$, $h'(t)$, $h''(t)$, …, $h^{(m-1)}(t)$ are continuous on the interval $[0, \infty)$ and of exponential order, while $\partial^\beta / \partial t^\beta [h(t)]$ if order α is piecewise continuous on the interval $[0, \infty)$, then the Laplace transform of the Caputo fractional derivative of $h(t)$ is expressed as

$$\mathcal{L}\left\{\frac{\partial^\beta}{\partial t^\beta} h(t)\right\} = p^\beta \mathcal{L}\{h(t)\} - \sum_{k=0}^{m-1} p^{\beta-k-1}\, h^{(k)}(0). \tag{36}$$

Because of the above equation and the initial conditions appearing in Eqs. (27), we get the parameter ψ according to the fraction theory used in the following form:

iv) The simple fractional derivative thermoelasticity (FD (s)) theory:

$$\psi = p\left(1 + \frac{\tau^\beta}{\beta!} p^\beta\right). \tag{37}$$

v) The simple fractional order of Lord and Shulman thermoelasticity (F-LS (s)) theory:

$$\psi = p\left(1 + \frac{\tau^{1+\beta}}{(1+\beta)!} p^{1+\beta}\right). \tag{38}$$

vi) The refined fractional order of Lord and Shulman thermoelasticity (LS (r)) theory:

$$\psi = p\left(1 + \sum_{n=1}^{N} \frac{\tau^{n+\beta}}{(n+\beta)!} p^{n+\beta}\right), \quad N > 1. \tag{39}$$

5. Solution of the problem and inverse Laplace transform

The solution of the physical field can be put in the Laplace domain in the following form:

$$\bar{\phi}(r) = \frac{\xi}{c_1}[A_1 J_0(\xi r) + A_2 Y_0(\xi r)] + A_{41} + c_5 r^2 + c_6, \tag{40}$$

$$\bar{s}(r) = A_1 J_1(\xi r) + A_2 Y_1(\xi r) + \frac{A_3}{r} + A_{42} r + c_7 r^3, \tag{41}$$

where A_j $(j = 1,2,3,4)$ are the integration constants, $J_0(\xi r)$, $J_1(\xi r)$ are Bessel's functions of the first kind of orders 0 and 1; $Y_0(\xi r)$, $Y_1(\xi r)$ are Bessel's functions of the second kind of orders 0 and 1, and

$$\begin{gathered} \xi^2 = -(c_3 + c_1 c_4), \quad A_{41} = -\frac{c_4}{\xi^2 c_3} A_4, \quad A_{42} = \frac{1}{2\xi^2}\left(A_4 - \frac{2c_2 c_3}{\xi^2}\right), \\ c_5 = -\frac{c_2 c_4}{2\xi^2}, \quad c_6 = \frac{2c_2 c_4 (c_3 - \xi^2)}{\xi^4 c_3}, \quad c_7 = \frac{c_2 c_3}{8\xi^2}. \end{gathered} \tag{42}$$

It is interesting to get the dilatation in Eq. (22) with the aid of the above solutions in the form

$$\bar{\varepsilon}(r) = c_8[A_1 J_0(\xi r) + A_2 Y_0(\xi r)] + c_9 A_4 + c_{10} r^2 + c_{11}, \tag{43}$$

where

$$\begin{gathered} c_8 = \frac{(1+\nu)\xi[c_1(1-2\nu) - 2\alpha E]}{c_1 E}, \quad c_9 = \frac{(1+\nu)[c_3(1-2\nu) + 2\alpha c_4 E]}{\xi^2 c_3 E}, \\ c_{10} = \frac{(1+\nu)\left[(1-2\nu)(4c_4 + \rho\omega^2) - 2\alpha c_5 E\right]}{E}, \quad c_{11} = -\frac{2(1+\nu)\left[(1-2\nu)c_2 c_3 + \alpha\xi^4 c_6 E\right]}{\xi^4 E}. \end{gathered} \tag{44}$$

The radial and hoop stresses may be obtained in the Laplace domain in the form

$$\bar{\sigma}_r(r) = \frac{1}{r}[A_1 J_1(\xi r) + A_2 Y_1(\xi r)] + \frac{A_3}{r^2} + \frac{A_4}{2\xi^2} + c_7 r^2 + c_{13}, \tag{45}$$

$$\bar{\sigma}_\theta(r) = \left[\xi J_0(\xi r) - \frac{1}{r} J_1(\xi r)\right] A_1 + \left[\xi Y_0(\xi r) - \frac{1}{r} Y_1(\xi r)\right] A_2 - \frac{A_3}{r^2} + \frac{A_4}{2\xi^2} + c_{12} r^2 + c_{13}, \tag{46}$$

where

$$c_{12} = 3c_7 + \rho\omega^2, \quad c_{13} = -\frac{c_2 c_3}{\xi^4}. \tag{47}$$

In addition, the axial stress σ_z can be obtained by using Eq. (14) with the aid of the temperature and the above stresses in the form

$$\bar{\sigma}_z(r) = \check{A}_1 J_0(\xi r) + \check{A}_2 Y_0(\xi r) + c_{14} A_4 + c_{15} r^2 + c_{16}, \tag{48}$$

where

$$\begin{gathered} \{\check{A}_1, \check{A}_2\} = \xi \left(\frac{\alpha E}{c_1} + \nu\right)\{A_1, A_2\}, \quad c_{14} = \frac{\nu c_3 - \alpha c_4 E}{\xi^2 c_3}, \\ c_{15} = \alpha c_5 E + \nu(c_7 + c_{12}), \quad c_{16} = \alpha E c_6 + 2\nu\, c_{13}. \end{gathered} \tag{49}$$

Once again, one can determine the radial displacement of the rotating cylinder in the Laplace domain by using dilatation in Eq. (43) in the form

$$\mathcal{D}_1(\bar{u}_r) = c_8[A_1 J_0(\xi r) + A_2 Y_0(\xi r)] + c_9 A_4 + c_{10} r^2 + c_{11}, \tag{50}$$

and its solution yields

$$\bar{u}_r = \frac{c_5}{\xi}[A_1 J_1(\xi r) + A_2 Y_1(\xi r)] + \frac{r}{2}(c_9 A_4 + c_{11}) + \frac{1}{4} c_{10} r^3 + \frac{A_5}{r}, \tag{51}$$

where A_5 is an additional constant.

6. Applications

The boundary conditions (23), (24), and (26) in the Laplace transform domain can be obtained as

$$\begin{gathered} \bar{\phi}(a,p) = 0, \quad \bar{\phi}(b,p) = \bar{G}(p) = \frac{\phi_0\left(1 - e^{-t_0 p}\right)}{t_0 p^2}, \\ \bar{\sigma}_r(a,p) = \bar{\sigma}_r(b,p) = 0, \quad \left.\frac{\partial \bar{u}_r(r,p)}{\partial r}\right|_{r=a} = 0. \end{gathered} \tag{52}$$

Using the above conditions, the parameters A_j, $j = 1,2,\ldots,5$ will be obtained from the following simultaneous equations

$$A_1 J_0(\xi a) + A_2 Y_0(\xi a) - c_{17} A_4 = q_1, \tag{53}$$

$$A_1 J_0(\xi b) + A_2 Y_0(\xi b) - c_{17} A_4 = q_2, \tag{54}$$

$$A_1 J_1(\xi a) + A_2 Y_1(\xi a) + p_1 A_3 + p_2 A_4 = q_3, \tag{55}$$

$$A_1 J_1(\xi b) + A_2 Y_1(\xi b) + p_3 A_3 + p_4 A_4 = q_4, \tag{56}$$

$$[\xi a J_0(\xi a) - J_1(\xi a)]A_1 + [\xi a Y_0(\xi a) - Y_1(\xi a)]A_2 + p_5 A_4 + p_6 A_5 = q_5, \tag{57}$$

where the parameter q_j and p_j are expressed as

$$\begin{gathered} \{q_1, q_2\} = \frac{c_1}{\xi}(\{0, \bar{G}(p)\} - c_5\{a^2, b^2\} - c_6), \quad \{p_1, p_3\} = \left\{\frac{1}{a}, \frac{1}{b}\right\}, \\ \{q_3, q_4\} = -\{a, b\}(\{a^2, b^2\}c_7 + c_{13}), \quad \{p_2, p_4\} = \frac{1}{2\xi^2}\{a, b\}, \\ q_5 = -\frac{\xi a\left(3c_{10}a^2 + 2c_{11}\right)}{4c_5}, \quad p_5 = \frac{\xi a c_9}{2c_5}, \quad p_6 = -\frac{\xi}{a c_5}, \quad c_{17} = \frac{c_1 c_4}{\xi^3 c_3}. \end{gathered} \tag{58}$$

Solving the above system of simultaneous equations provides the parameters A_j. With the aid of these parameters, one can determine all field quantities of the rotating cylinder in the Laplace domain. To obtain the solutions in the physical realm, we should view the function $f(r,t)$ as an inversion of the Laplace transform $\bar{f}(r,s)$ by using the formula

$$f(r,t)=\mathcal{L}^{-1}\{f(r,s)\}=\frac{e^{\upsilon t}}{t}\left\{\frac{1}{2}\bar{f}(r,\upsilon)+\mathrm{Re}\left[\sum_{m=1}^{M}(-1)^m\bar{f}\left(r,\upsilon+\frac{im\pi}{t}\right)\right]\right\}, \tag{59}$$

where $i=\sqrt{-1}$ and Re is the real part. The physical quantities (temperature ϕ, displacement u_r, stresses σ_r, σ_θ, dilatation ε) are decomposed using a series expansion with a large integer M and an arbitrary constant υ. The empirical relation $\upsilon t\approx 4.7$ [51] is used to speed up computations.

7. Numerical outcomes and discussions

Laplace-domain solutions are inverted back to the time domain to obtain results according to all models. Copper is used as the material with the following given constants:

$$\begin{gathered}\lambda=7.76\times10^{10}\ (\mathrm{kg\,m^{-1}\,s^{-2}}),\quad \mu=3.86\times10^{10}\ (\mathrm{kg\,m^{-1}\,s^{-2}}),\\ \rho=8954\ (\mathrm{kg\,m^{-3}}),\quad c_\vartheta=383.1\ (\mathrm{J\,kg^{-1}\,K^{-1}}),\quad \alpha=1.78\times10^{-5}\ (\mathrm{K^{-1}}),\\ \kappa=386\ (\mathrm{W\,m^{-1}\,K^{-1}}),\quad T_0=293\ \mathrm{K}.\end{gathered} \tag{60}$$

Young's modulus E and Poisson's ratio ν will be given by using the well-known formulae between them and Lame's constants

$$E=\frac{\mu(3\lambda+2\mu)}{\lambda+\mu},\quad \nu=\frac{\lambda}{2(\lambda+\mu)}. \tag{61}$$

Some key parameters like $\tau=0.05$, $\phi_0=10^8$, and $\omega=100$ are used. Results are computed for both fractional and non-fractional thermoelasticity theories and illustrated in Figures 2–12.

7.1 Comparison between various theories

Figures 2-6 show the temperature ϕ, the radial displacement u_r, the dilatation ε, the radial stress σ_r, and the hoop stress σ_θ along the radial direction of the rotating cylinder employing the refined fractional order of Lord and Shulman thermoelasticity theory (LS (r)), the simple fractional order of Lord and Shulman thermoelasticity theory (F-LS (s)), the simple fractional derivative thermoelasticity theory (FD (s)), the refined Lord and Shulman thermoelasticity theory (LS (r)), the simple Lord and Shulman thermoelasticity theory (LS (s)), and the classical thermoelasticity theory (CTE). Such figures compare the field variables across the radius of a cylinder (from the center, $r=1$, to the outer surface, $r=1$) for different thermoelastic theories and under different fractional orders.

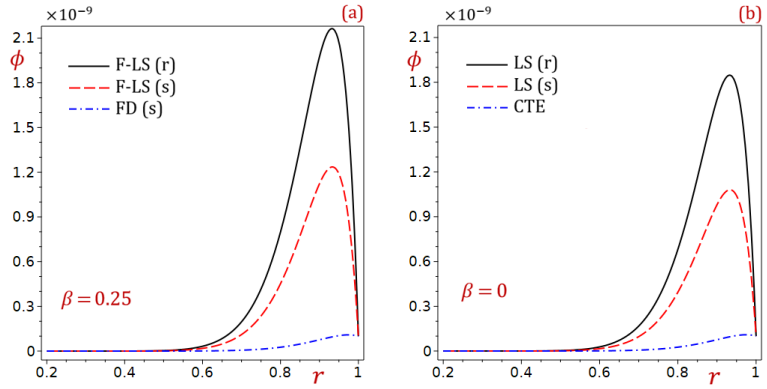

Fig 2: The temperature ϕ of the cylinder with and without fraction parameter (a) $\beta=0.25$ (b) $\beta=0$

As shown in Fig. 2, the temperature distribution ϕ exhibits a consistent behavioral trend along the radial direction of the rotating cylinder, both with and without the inclusion of the fractional parameter β. Figure 2(a), with $\beta=0.25$, demonstrates that the inclusion of the fractional parameter results in a significantly higher magnitude of temperature ϕ across the entire radius compared to the theories without it, as in Fig. 2(b). Furthermore, the choice of thermoelastic

theory has a notable impact on the temperature profile. The refined fractional Lord-Shulman (F-LS (r)) and simple fractional Lord-Shulman (F-LS (s)) theories predict the highest temperatures, while the simple fractional derivative (FD (s)) theory predicts a lower magnitude. Figure 2(b), with $\beta = 0$, shows that for the classical and non-fractional Lord-Shulman theories, the temperature ϕ increases monotonically with the radius r. The refined theory (LS (r)) predicts the highest temperature, followed by the simple theory (LS (s)), with the classical theory (CTE) predicting the lowest values. In $0.6 \leq r < 0.1$, the temperature ϕ is no longer increasing. The maximum values are achieved at $r = 0.93$ for the refined theory, at $r = 0.94$ for the simple theory, and at $r = 0.975$ for the classical theory.

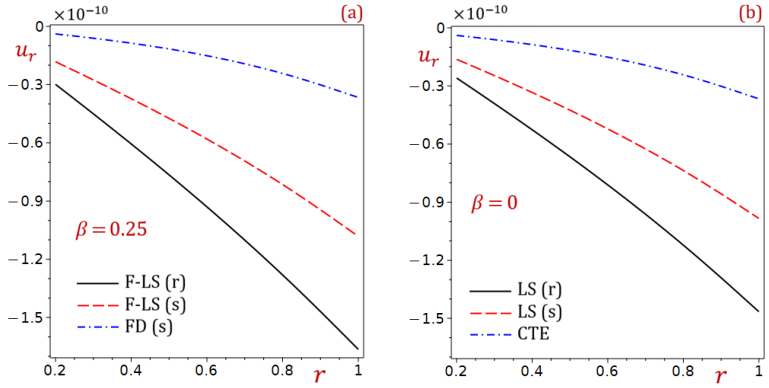

Fig 3: The radial displacement u_r of the cylinder with and without fraction parameter (a) $\beta = 0.25$ (b) $\beta = 0$

Based on Fig. 3, the radial displacement u_r is negative and its magnitude (absolute value) increases along the radial direction of the rotating cylinder, indicating an inward displacement towards the center. The displacement does not decrease linearly. The curves are concave, showing a non-linear increase in magnitude (becoming more negative) with radius r. The rate of change is higher in the inner region and moderates towards the outer boundary. Comparing Fig. 3(a) ($\beta = 0.25$) to Fig. 3(b) ($\beta = 0$) shows that the inclusion of the fractional parameter β results in significantly larger magnitude displacements (more negative values). The entire displacement field in Fig. 3(a) is shifted down compared to Fig. 3(b). The description of the location of maximum and minimum displacement is reversed. The maximum (least negative) displacement occurs at the inner surface $r = 0$. The minimum (most negative) displacement, or largest magnitude inward motion, occurs on the outer surface $r = 1$. The radial displacement is very sensitive to the change in the thermoelasticity theories. In both plots, the three theories yield distinct results. The refined theories (F-LS (r) and LS (r)) consistently predict the largest magnitude displacements (most negative values), while the classical theory (CTE) and simple fractional derivative theory (FD (s)) predict the smallest magnitudes.

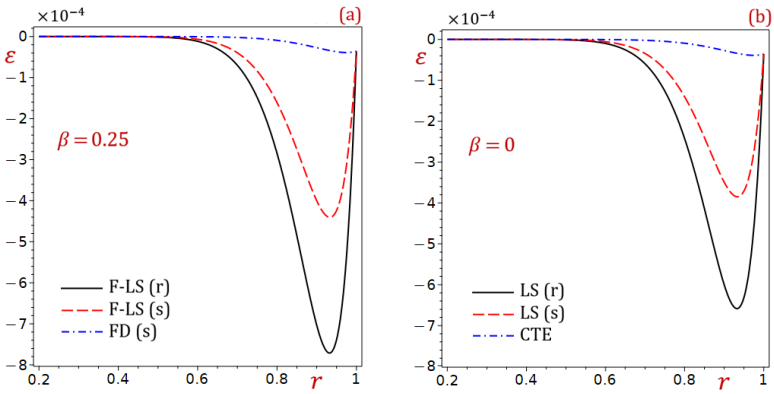

Fig 4: The dilatation ε of the cylinder with and without fraction parameter (a) $\beta = 0.25$ (b) $\beta = 0$

Figure 4 shows that the dilatation ε is negative and its behavior is highly sensitive to both the inclusion of the fractional parameter β and the choice of thermoelastic theory. The magnitude of the (negative) dilatation is significantly larger in the fractional case (Fig. 4a, $\beta = 0.25$) than in the non-fractional case (Fig. 4b, $\beta = 0$). The inclusion of β increases the volumetric compression. The dilatation ε becomes more negative (increases in magnitude)

with increasing radius r, reaches a minimum (point of maximum compression), and then becomes less negative (decreases in magnitude) as it approaches the outer boundary. For $\beta = 0.25$ (Fig. 4a), this minimum occurs at an interior point for all three theories. The simple refined theory (F-LS (s, r)) has its minimum around $r \approx 0.93$, while the simple fractional derivative theory (FD (s)) has its minimum closest to the outer edge. The same may occur in Fig. 4b. The three lines for each value of β are distinct and separate across the entire domain, including the interval from $r = 0.2$ to $r = 0.6$. The theories are differentiable everywhere, though the difference between them may become more pronounced at larger radii.

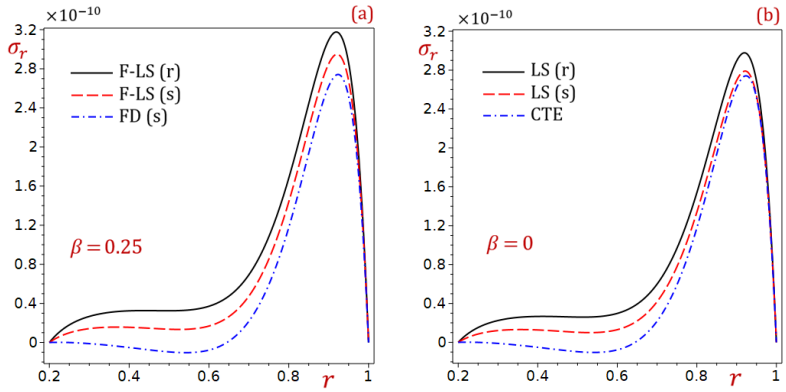

Fig 5: The radial stress σ_r in the cylinder with and without fraction parameter (a) $\beta = 0.25$ (b) $\beta = 0$

Figure 5 shows the distribution of radial stress σ_r, which is tensile and sensitive to both the fractional parameter β and the thermoelastic theory used. The stress is zero at the inner and outer surfaces, rising to a maximum at an interior point. The inclusion of the fractional parameter β significantly increases the magnitude of the stress. The refined theories (F-LS (r) and LS (r)) predict the highest stress values, although the exact location of the peak stress varies with the theory and the value of β. Simple and classical theories predict lower stresses and a peak location closer to the outer boundary. Overall, the presence of β leads to substantially higher radial stresses.

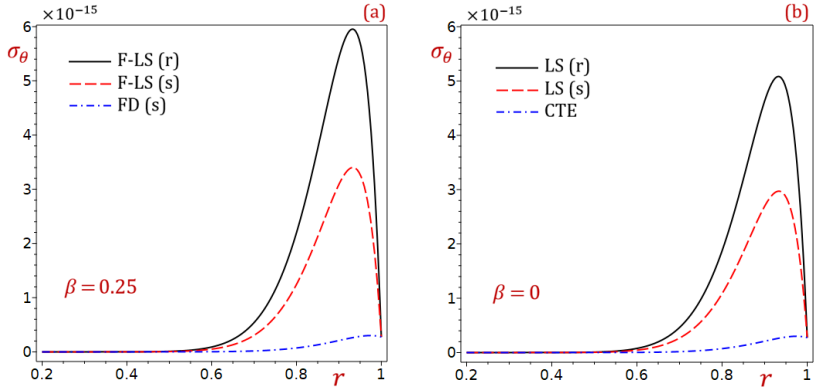

Fig 6: The hoop stress σ_θ in the cylinder with and without fraction parameter (a) $\beta = 0.25$ (b) $\beta = 0$

Based on Fig. 6, the hoop stress σ_θ is tensile (positive) and its distribution is significantly influenced by both the fractional parameter β and the choice of thermoelastic theory. The inclusion of the fraction parameter causes high hoop stresses. The magnitude of the hoop stress is dramatically higher in the fractional case (Fig. 6a, $\beta = 0.25$) by an order of magnitude compared to the non-fractional case (Fig. 6b, $\beta = 0$). For all cases, the hoop stress increases from the inner edge, reaches a maximum at an interior point, and then decreases. The simple and refined theory (F-LS (s, r)) peaks around $r \approx 0.91$, and the simple fractional derivative theory (FD (s)) has its maximum closest to the outer edge. The curves of σ_θ for each value of β are separate and distinct across the entire domain, including the interval from $r = 0.2$ to $r = 0.6$. The difference is more pronounced at larger radii, but the theories are differentiable everywhere.

7.2 Effect of fractional parameter β

The graphs of temperature, displacement, dilatation, and stresses are contrived in Figures 7-11 along the radial direction of the rotating cylinder using the refined LS theory with $N > 1$. Three values of the fractional parameter $\beta = 0$, 0.2, and 0.5. The refined fractional order of Lord and Shulman thermoelasticity theory (LS (r)) may tend to the refined Lord and Shulman thermoelasticity theory (LS (r)) by setting $\beta = 0$. The temperature ϕ and stresses σ_r and σ_θ increase with the increase in the fractional parameter β as shown in Figures 7, 10, and 11. However, the radial displacement and dilatation decrease with the increase in the fractional parameter β, as shown in Figures 8 and 9.

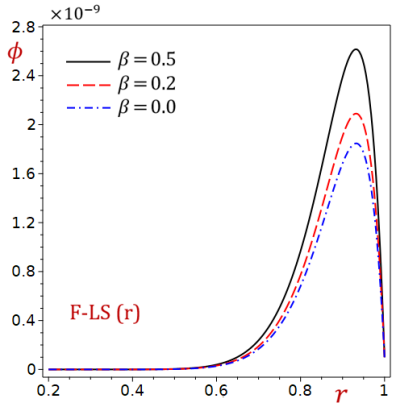

Fig 7: Effect of fractional parameter β on the temperature ϕ of the cylinder due to the refined F-LS (r) theory

Based on Fig. 7, the temperature distribution ϕ within the cylinder is highly sensitive to the value of the fractional parameter β when using the refined F-LS (r) theory. The graph demonstrates that increasing the fractional parameter β causes a significant increase in the magnitude of the temperature ϕ across the entire radial domain. The temperature profile for the largest parameter ($\beta = 0.5$) is markedly higher than for the intermediate value ($\beta = 0.2$), which in turn is higher than the profile for the classical case ($\beta = 0$). Furthermore, the shape of the temperature curve remains consistent for all values of β. It increases from the center, reaches a maximum value at an interior point ($r \approx 0.91$), and then decreases towards the outer boundary ($r = 1$). The value of β does not appear to significantly alter the radial location of this maximum temperature.

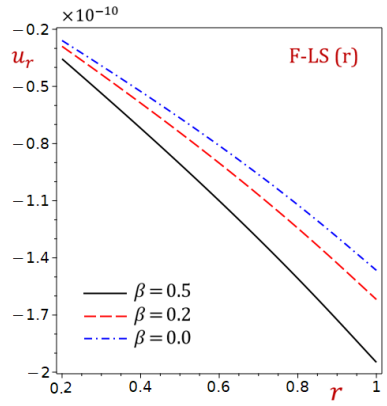

Fig 8: Effect of fractional parameter β on the radial displacement u_r of the cylinder due to the refined F-LS (r) theory

Based on Fig. 8, the radial displacement u_r within the cylinder is significantly influenced by the value of the fractional parameter β according to the refined F-LS (r) theory. The graph shows that increasing the fractional parameter β results in a less negative (smaller in magnitude) radial displacement u_r across the entire radius. The displacement is negative, indicating an inward motion towards the center.

The curve for the classical case ($\beta = 0.0$) is the closest to zero, followed by the intermediate value ($\beta = 0.2$), while the largest parameter ($\beta = 0.5$) exhibits the most negative displacement (largest magnitude inward). The overall shape

of the displacement profile remains consistent for all values of β, decreasing (becoming more negative) from the center until reaching a minimum at the outer boundary.

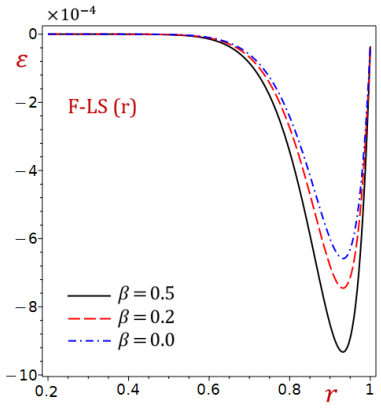

Fig 9: Effect of fractional parameter β on the dilatation ε of the cylinder due to the refined F-LS (r) theory

Figure 9 shows that the dilatation ε (volumetric strain) within the cylinder is significantly affected by the value of the fractional parameter β according to the refined F-LS (r) theory. The graph shows that increasing the fractional parameter β results in a less negative (smaller in magnitude) dilatation ε across the entire radius. The dilatation is negative for all cases, indicating a volumetric compression.

The curve for the classical case ($\beta = 0$) is the closest to zero, followed by the intermediate value ($\beta = 0.2$), while the largest parameter ($\beta = 0.5$) exhibits the most negative dilatation (largest magnitude of compression). The overall shape of the dilatation profile is consistent for all values of β, decreasing (becoming more negative) from the center until reaching a minimum around $r \approx 0.93$, before increasing slightly towards the outer boundary.

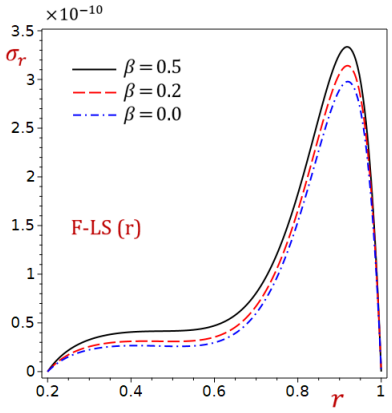

Fig 10: Effect of fractional parameter β on the radial stress σ_r in the cylinder due to the refined F-LS (r) theory

Based on Fig. 10, the radial stress σ_r within the cylinder is significantly influenced by the value of the fractional parameter β according to the refined F-LS (r) theory. The graph shows that increasing the fractional parameter β results in an increase in the magnitude of the radial stress σ_r across the entire radius. The radial stress is positive (tensile) for all cases.

The curve for the classical case ($\beta = 0$) has the lowest magnitude, followed by the intermediate value ($\beta = 0.2$), while the largest parameter ($\beta = 0.5$) exhibits the highest tensile stress. The overall shape of the stress profile is consistent for all values of β, increasing from zero at the center ($r = 0$), reaching a maximum value at $r \approx 0.9$, and then decreasing back to zero at the free outer boundary ($r = 1$), as expected. The value of β affects the peak stress level but not the fundamental shape of the distribution.

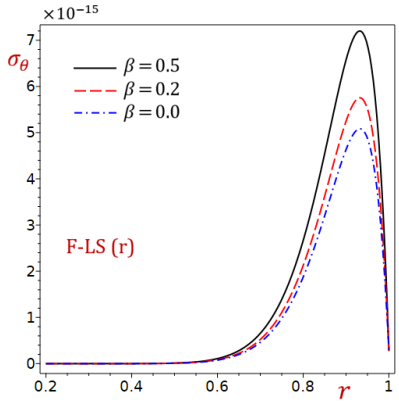

Fig 11: Effect of fractional parameter β on the hoop stress σ_θ in the cylinder due to the refined F-LS (r) theory

Based on Fig. 11, the hoop stress σ_θ within the cylinder is significantly influenced by the value of the fractional parameter β according to the refined F-LS (r) theory. The graph shows that increasing the fractional parameter β results in a substantial increase in the magnitude of the hoop stress σ_θ across the entire radius. The hoop stress is positive (tensile) for all cases.

The curve for the classical case ($\beta = 0$) has the lowest magnitude, followed by the intermediate value ($\beta = 0.2$), while the largest parameter ($\beta = 0.5$) exhibits the highest tensile stress. The overall shape of the stress profile is consistent for all values of β, starting from a positive value at the center, increasing to a maximum, and then decreasing. The value of β significantly affects the peak stress level but not the fundamental shape of the distribution.

7.3 Effect of ramp-type heating parameter t_0

The effect of the ramp-type heating parameter t_0 is studied in one example. Figure 12 shows the radial stress σ_r along the radial direction of the rotating cylinder for distinct values of the dimensionless time t utilizing the refined fractional order of Lord and Shulman thermoelasticity theory (LS (r)) and the refined Lord and Shulman thermoelasticity theory (LS (r)).

The radial stresses are very sensitive to the variation of the ramp-type heating parameter t_0. They increase as t_0 decreases. The inclusion of the fractional parameter β causes high stresses.

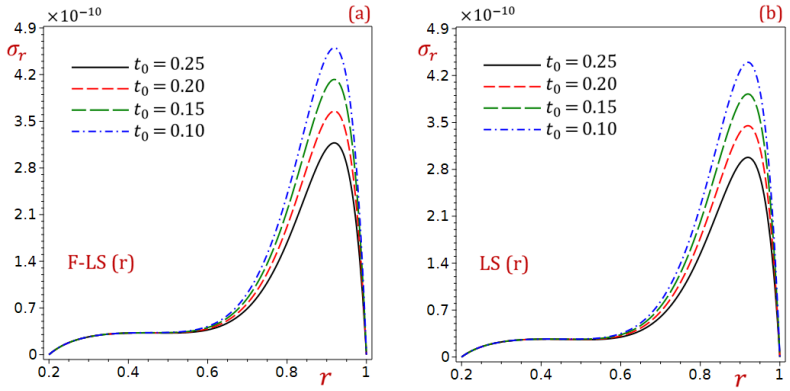

Fig 12: Effect of ramp-type heating parameter t_0 on the radial stress σ_r of the cylinder with and without fraction parameter (a) $\beta = 0.25$ (b) $\beta = 0$

Based on Fig. 12, the radial stress σ_r is significantly influenced by the ramp-time heating parameter t_0 in both fractional and non-fractional thermoelasticity theories. A key general conclusion is that the fractional parameter β dramatically amplifies the sensitivity of the stress response to changes in the thermal loading time t_0.

In Fig. 12(a), increasing the ramp-time parameter t_0 (slower heating) causes a significant decrease in the magnitude of the radial stress σ_r. The stresses are notably higher for faster heating (e.g., $t_0 = 0.1$) and lower for slower heating

(e.g., $t_0 = 0.25$). The shape of the stress distribution curve remains consistent, but is scaled down in magnitude as t_0 increases.

In Fig. 12(b), increasing the ramp-time parameter t_0 also causes a decrease in the radial stress σ_r, but the effect is much less pronounced compared to the fractional case. The range of stress values for different t_0 is much narrower. The curves for different t_0 values are clustered closer together. Similar to Fig. 12(a), the fundamental shape of the stress curve is preserved, showing that the effect of t_0 is primarily on the magnitude.

The presence of the fractional parameter β intensifies the system's dependence on the rate of thermal loading. The radial stress becomes far more sensitive to changes in the ramp-time heating parameter t_0 when fractional calculus is incorporated ($\beta > 0$) into the refined Lord-Shulman theory. This demonstrates that fractional models capture a more complex and rate-dependent thermoelastic response, where the history of the thermal load has a greater impact on the resulting stress field. In contrast, the classical non-fractional theory ($\beta = 0$) predicts a stress field that is less sensitive to the speed of the applied heating.

8. Conclusions

The provided article discusses the results of a study analyzing the thermoelastic behavior of a rotating cylinder using the refined Lord-Shulman (LS) theory with a fractional order parameter β and the ramp-time heating t_0. The effects of fractional parameter β and thermoelasticity theories (classical, simple, refined) on temperature, displacement, stresses, and dilatation in a rotating cylinder. The temperature ϕ increased with β but followed the same radial trend and some peaks at different radial positions depending on the theory discussed. The radial displacement u_r decreased linearly from inner to outer surfaces. Smaller displacements occur when β is included with highly sensitive to the choice of thermoelastic theory. The dilatation ε is lower with β inclusion and reaches minimum values at different radial positions according to the used theory. The radial stress σ_r showed the highest values in refined theories and peaked around $r \approx 0.92$. This stress increases with β inclusion and vanishes at cylinder boundaries. The hoop stress σ_θ decreased with β inclusion and peaked at similar positions as temperature. The temperature ϕ, radial stress σ_r, and hoop stress σ_θ are increased as β increases. This suggested that fractional order effects amplify thermal and mechanical stresses. The radial displacement and dilatation are decreased with increasing β. This indicates that fractional damping reduces deformation. For $\beta = 0$ the refined fractional LS theory reduces to the classical refined LS theory. Finally, the radial stress σ_r increased when the ramp-time heating t_0 decreases (faster heating) and the fractional parameter β further increases the stress magnitudes.

The implications of the present study can be summarized. The fractional parameter β introduces memory-dependent effects, influencing thermoelastic responses. Smaller t_0 (rapid heating) leads to higher stresses, which is critical in applications like thermal shock analysis. The refined fractional LS model provides a more generalized framework compared to the classical LS theory (when $\beta = 0$). Also, the potential applications of the present study may appear in high-speed rotating systems (e.g., turbine blades, flywheels). The thermal stress management in functionally graded materials. Design optimization under transient heating conditions.

References

[1] M. A. Biot, Thermoelasticity and Irreversible Thermodynamics, *Journal of Applied Physics,* Vol. 27, No. 3, pp. 240-253, 1956.

[2] Y. Yu-Ching, C. Cha'o-Kuang, Thermoelastic transient response of an infinitely long annular cylinder composed of two different materials, *International Journal of Engineering Science,* Vol. 24, No. 4, pp. 569-581, 1986/01/01/, 1986.

[3] Z. Y. L. K. C. Jane, THERMOELASTICITY OF MULTILAYERED CYLINDERS, *Journal of Thermal Stresses,* Vol. 22, No. 1, pp. 57-74, 1999/02/01, 1999.

[4] Z. Y. Lee, C. K. Chen, C. I. Hung, Transient thermal stress analysis of multilayered hollow cylinder, *Acta Mechanica,* Vol. 151, No. 1, pp. 75-88, 2001/03/01, 2001.

[5] Z.-Y. Lee, Generalized coupled transient response of 3-D multilayered hollow cylinder, *International Communications in Heat and Mass Transfer,* Vol. 33, No. 8, pp. 1002-1012, 2006/10/01/, 2006.

[6] P. B. Gaikwad, K. R. Gaikwad, K. P. Ghadle, Study of an exact solution of steady-state thermoelastic problem of a finite length hollow cylinder, *International Journal of Computational and Applied Mathematics,* Vol. 5, pp. 177+, 2010/03//

//, 2010. English

[7] A. M. Zenkour, D. S. Mashat, K. A. Elsibai, Bending Analysis of Functionally Graded Plates in the Context of Different Theories of Thermoelasticity, *Mathematical Problems in Engineering,* Vol. 2009, No. 1, pp. 962351, 2009.

[8] Y. Tokovyy, O. Hrytsyna, M. Hrytsyna, Thermoelastic response of multilayer cylinders: The direct integration and single-solid approach, *Journal of Thermal Stresses,* Vol. 47, No. 6, pp. 841-857, 2024/06/02, 2024.

[9] M. Eskandari-Ghadi, M. Rahimian, A. Mahmoodi, A. Ardeshir-Behrestaghi, Analytical Solution for Two-Dimensional Coupled Thermoelastodynamics in a Cylinder, *Civil Engineering Infrastructures Journal,* Vol. 46, No. 2, pp. 107-123, 2013.

[10] A. M. Zenkour, I. A. Abbas, Nonlinear Transient Thermal Stress Analysis of Temperature-Dependent Hollow Cylinders Using a Finite Element Model, *International Journal of Structural Stability and Dynamics,* Vol. 14, No. 07, pp. 1450025, 2014.

[11] H. W. Lord, Y. Shulman, A generalized dynamical theory of thermoelasticity, *Journal of the Mechanics and Physics of Solids,* Vol. 15, No. 5, pp. 299-309, 1967/09/01/, 1967.

[12] R. S. Dhaliwal, H. H. Sherief, GENERALIZED THERMOELASTICITY FOR ANISOTROPIC MEDIA, *Quarterly of Applied Mathematics,* Vol. 38, No. 1, pp. 1-8, 1980.

[13] H. H. Sherief, M. N. Anwar, A problem in generalized thermoelasticity for an infinitely long annular cylinder, *International Journal of Engineering Science,* Vol. 26, No. 3, pp. 301-306, 1988/01/01/, 1988.

[14] H. M. Youssef, GENERALIZED THERMOELASTICITY OF AN INFINITE BODY WITH A CYLINDRICAL CAVITY AND VARIABLE MATERIAL PROPERTIES, *Journal of Thermal Stresses,* Vol. 28, No. 5, pp. 521-532, 2005/05/01, 2005.

[15] H. M. Youssef, Problem of generalized thermoelastic infinite medium with cylindrical cavity subjected to a ramp-type heating and loading, *Archive of Applied Mechanics,* Vol. 75, No. 8, pp. 553-565, 2006/05/01, 2006.

[16] E. Marchi, G. Zgrablich, Heat Conduction in Hollow Cylinders with Radiation, *Proceedings of the Edinburgh Mathematical Society,* Vol. 14, No. 2, pp. 159-164, 1964.

[17] H. M. Youssef, Generalized thermoelastic infinite medium with cylindrical cavity subjected to moving heat source, *Mechanics Research Communications,* Vol. 36, No. 4, pp. 487-496, 2009/06/01/, 2009.

[18] S. M. Abo-Dahab, I. A. Abbas, LS model on thermal shock problem of generalized magneto-thermoelasticity for an infinitely long annular cylinder with variable thermal conductivity, *Applied Mathematical Modelling,* Vol. 35, No. 8, pp. 3759-3768, 2011/08/01/, 2011.

[19] M. A. Elhagary, Generalized thermoelastic diffusion problem for an infinitely long hollow cylinder for short times, *Acta Mechanica,* Vol. 218, No. 3, pp. 205-215, 2011/05/01, 2011.

[20] A. M. Zenkour, I. A. Abbas, A generalized thermoelasticity problem of an annular cylinder with temperature-dependent density and material properties, *International Journal of Mechanical Sciences,* Vol. 84, pp. 54-60, 2014/07/01/, 2014.

[21] I. A. Abbas, Y. A. elmaboud, Analytical solutions of thermoelastic interactions in a hollow cylinder with one relaxation time, *Mathematics and Mechanics of Solids,* Vol. 22, No. 2, pp. 210-223, 2017.

[22] A. M. Zenkour, Generalized Thermoelasticity Theories for Axisymmetric Hollow Cylinders Under Thermal Shock with Variable Thermal Conductivity, *Journal of Molecular and Engineering Materials,* Vol. 06, No. 03n04, pp. 1850006, 2018.

[23] H. M. Youssef, A. A. El-Bary, Characterization of the photothermal interaction on a viscothermoelastic semiconducting solid cylinder due to rotation under Lord-Shulman model, *Alexandria Engineering Journal,* Vol. 60, No. 2, pp. 2083-2092, 2021/04/01/, 2021.

[24] M. Eker, D. Yarımpabuç, A Generalized Thermoelastic Behaviour of Isotropic Hollow Cylinder, *Türk Doğa ve Fen Dergisi,* Vol. 11, No. 3, pp. 123-128, September, 2022. en

[25] A. E. Green, K. A. Lindsay, Thermoelasticity, *Journal of Elasticity,* Vol. 2, No. 1, pp. 1-7, 1972/03/01, 1972.

[26] A. E. Green, P. M. Naghdi, A Re-Examination of the Basic Postulates of Thermomechanics, *Proceedings of the Royal Society of London Series A,* Vol. 432, pp. 171-194, February 01, 1991, 1991.

[27] A. E. Green, P. M. Naghdi, ON UNDAMPED HEAT WAVES IN AN ELASTIC SOLID, *Journal of Thermal Stresses,* Vol. 15, No. 2, pp. 253-264, 1992/04/01, 1992.

[28] A. E. Green, P. M. Naghdi, Thermoelasticity without energy dissipation, *Journal of Elasticity,* Vol. 31, No. 3, pp. 189-208, 1993/06/01, 1993.

[29] M. N. Allam, K. A. Elsibai, A. E. AbouElregal, THERMAL STRESSES IN A HARMONIC FIELD FOR AN INFINITE BODY WITH A CIRCULAR CYLINDRICAL HOLE WITHOUT ENERGY DISSIPATION, *Journal of Thermal Stresses,* Vol. 25, No. 1, pp. 57-67, 2002/01/01, 2002.

[30] A. M. Zenkour, A. E. Abouelregal, Effect of temperature dependency on constrained orthotropic unbounded body with a cylindrical cavity due to pulse heat flux, *Journal of Thermal Science and Technology,* Vol. 10, No. 1, pp. JTST0019-JTST0019, 2015.

[31] A. M. Zenkour, M. A. Kutbi, Multi thermal relaxations for thermodiffusion problem in a thermoelastic half-space, *International Journal of Heat and Mass Transfer,* Vol. 143, pp. 118568, 2019/11/01/, 2019.

[32] M. I. A. Othman, I. A. Abbas, Thermal shock problem in a homogeneous isotropic hollow cylinder with energy dissipation, *Computational Mathematics and Modeling,* Vol. 22, No. 3, pp. 266-277, 2011/07/01, 2011.

[33] S. Bezzina, A. M. Zenkour, Thermoelastic diffusion of a solid cylinder in the context of modified Green–Naghdi models, *Waves in Random and Complex Media,* Vol. 34, No. 4, pp. 2476-2497, 2024/07/03, 2024.

[34] M. Othman, I. Abbas, Effect of Rotation on Magneto-Thermoelastic Homogeneous Isotropic Hollow Cylinder with Energy Dissipation Using Finite Element Method, *Journal of Computational and Theoretical Nanoscience,* Vol. 12, pp. 2399-2404, 09/01, 2015.

[35] A. M. Zenkour, M. A. Kutbi, Thermoelastic interactions in a hollow cylinder due to a continuous heat source without energy dissipation, *Materials Research Express,* Vol. 7, No. 3, pp. 035702, 2020/03/09, 2020.

[36] Y. Povstenko, Non-axisymmetric solutions to time-fractional diffusion-wave equation in an infinite cylinder, *Fractional Calculus and Applied Analysis,* Vol. 14, No. 3, pp. 418-435, 2011/09/01, 2011.

[37] H. Youssef, E. Al-lehaibi, Fractional Order Generalized Thermoelastic Infinite Medium with Cylindrical Cavity Subjected to Harmonically Varying Heat, *Engineering,* Vol. 3, pp. 32, 01/29, 2011.

[38] A. E. Abouelregal, Fractional heat conduction equation for an infinitely generalized, thermoelastic, long solid cylinder, *International Journal for Computational Methods in Engineering Science and Mechanics,* Vol. 17, No. 5-6, pp. 374-381, 2016/11/01, 2016.

[39] Khamis, Generalized thermoelasticity with fractional order strain of infinite medium with a cylindrical cavity, *International Journal of ADVANCED AND APPLIED SCIENCES*, 2020.

[40] S. M. Said, E. M. Abd-Elaziz, M. I. A. Othman, A two-temperature model and fractional order derivative in a rotating thick hollow cylinder with the magnetic field, *Indian Journal of Physics,* Vol. 97, No. 10, pp. 3057-3064, 2023/09/01, 2023.

[41] P. Xie, T. He, Investigation on the electromagneto-thermoelastic coupling behaviors of a rotating hollow cylinder with memory-dependent derivative, *Mechanics Based Design of Structures and Machines,* Vol. 51, No. 6, pp. 3119-3137, 2023/06/03, 2023.

[42] E. A. N. Al-Lehaibi, Generalized Thermoelastic Infinite Annular Cylinder under the Hyperbolic Two-Temperature Fractional-Order Strain Theory, *Fractal and Fractional,* Vol. 7, No. 6, pp. 476, 2023.

[43] M. I. A. Othman, H. M. Atef, Conformable Fractional Order Theory in Thermoelasticity, *Mechanics of Solids,* Vol. 59, No. 2, pp. 1180-1193, 2024/04/01, 2024.

[44] S. D. Warbhe, V. Gujarkar, Thermoelastic impact in a thick hollow cylinder using time-fractional-order theory, *Journal of Thermal Stresses,* Vol. 47, No. 2, pp. 263-274, 2024/02/01, 2024.

[45] H. Zhu, J. He, T. Zhu, Y. Yue, M. Chen, Analysis of a hollow cylinder with variable thermal conductivity and diffusivity by fractional thermoelastic diffusion theory, *Journal of Thermal Stresses,* Vol. 47, No. 8, pp. 1055-1072, 2024/08/02, 2024.

[46] M. Adel, A. El-Dali, M. A. Seddeek, A. S. Yahya, A. A. El-Bary, K. Lotfy, The Fractional Derivative and Moisture Diffusivity for Moore-Gibson-Thompson Model of Rotating Magneto-Semiconducting Material, *Journal of Vibration Engineering & Technologies,* Vol. 12, No. 1, pp. 233-249, 2024/12/01, 2024.

[47] H. H. Sherief, E. M. Hussein, New fractional order model of thermoporoelastic theory for a porous infinitely long cylinder saturated with fluid, *Waves in Random and Complex Media,* Vol. 34, No. 5, pp. 4754-4783, 2024/09/02, 2024.

[48] A. Zakria, A. E. Abouelregal, Fractional viscoelastic model with a non-singular kernel for a rotating semiconductor circular cylinder permeated by a magnetic field and due to heat flow pulse heating, *Waves in Random and Complex Media,* Vol. 35, No. 1, pp. 1955-1990, 2025/01/02, 2025.

[49] H. Wang, Y. Ma, Thermoelastic Response of an Infinite Hollow Cylinder under Fractional Order Dual-Phase-Lag Theory, *Mechanics of Solids,* Vol. 59, No. 1, pp. 459-482, 2024/02/01, 2024.

[50] S. E. Khader, A. A. Marrouf, M. Khedr, Application of the fractional-order theory of micropolar thermoelasticity in the solid cylinder, *Journal of the Brazilian Society of Mechanical Sciences and Engineering,* Vol. 46, No. 8, pp. 459, 2024/06/18, 2024.

[51] G. Honig, U. Hirdes, A method for the numerical inversion of Laplace transforms, *Journal of Computational and Applied Mathematics,* Vol. 10, No. 1, pp. 113-132, 1984/02/01/, 1984.